Υ

SLAC-PUB-2421
LBL-10016
October 1979
(T/E)

RESULTS ON TWO-PHOTON INTERACTIONS FROM MARK II AT SPEAR*

G. S. Abrams, M. S. Alam, C. A. Blocker, A. M. Boyarski, M. Breidenbach, D. L. Burke, W. C. Carithers, W. Chinowsky, M. W. Coles, S. Cooper, W. E. Dieterle, J. B. Dillon, J. Dorenbosch, J. M. Dorfan, M. W. Eaton, G. J. Feldman, M. E. B. Franklin, G. Gidal, G. Goldhaber, G. Hanson, K. G. Hayes, T. Himel, D. G. Hitlin†, R. J. Hollebeek, W. R. Innes, J. A. Jaros, P. Jenni, A. D. Johnson, J. A. Kadyk, A. J. Lankford, R. R. Larsen, V. Lüth, R. E. Millikan, M. E. Nelson, C. Y. Pang, J. F. Patrick, M. L. Perl, B. Richter, A. Roussarie, D. L. Scharre, R. H. Schindler, R. F. Schwitters‡, J. L. Siegrist, J. Strait, H. Taureg, V. I. Telnov§, M. Tonutti¶, G. H. Trilling, E. N. Vella, R. A. Vidal, I. Videau, J. M. Weiss, and H. Zaccone[θ]

Presented by Peter Jenni¶

Stanford Linear Accelerator Center¶
Stanford University, Stanford, California 94305

and

Lawrence Berkeley Laboratory and Department of Physics
University of California, Berkeley, California 94720

ABSTRACT

Preliminary results on two-photon interactions from the SLAC-LBL Mark II magnetic detector at SPEAR are presented. The cross section for η' production by the reaction $e^+e^- \rightarrow e^+e^-\eta'$ has been measured over the beam energy range from 2 to 4 GeV. The radiative width $\Gamma_{\gamma\gamma}(\eta')$ has been determined to be 5.8 ± 1.1 keV (±20% systematic uncertainty). Upper limits on the radiative widths of the f(1270), A_2(1310) and f'(1515) mesons have been determined.

* Work supported by the Department of Energy under contract numbers DE-AC03-76SF00515 and W-7405-ENG-48.
† California Institute of Technology, Pasadena, California 91125.
‡ Harvard University, Cambridge, Massachusetts 02138.
§ Institute of Nuclear Physics, Novosibirsk 90, USSR.
¶ Universität Bonn, F. R. Germany.
θ CEN-Saclay, France.

(Invited talk presented at the International Conference on Two-Photon Interactions, Lake Tahoe, California, August 30 - September 1, 1979.)

I. Introduction

In this talk we report some preliminary results on two-photon interactions from the Mark II experiment at the Stanford Linear Accelerator Center e^+e^- storage ring facility SPEAR. The basic diagram for the two-photon process is shown in Fig. 1. Lepton pairs produced by the two-photon process have been observed in several experiments[1-3] but only very few events with hadrons in the final state have been observed so far.[3,4] The first evidence of a meson resonance produced by the two-photon interaction has been reported recently by the Mark II collaboration;[5] the reaction

$$e^+e^- \rightarrow e^+e^-\eta'(958) \qquad (1)$$

has been observed by detecting the $\eta' \rightarrow \pi^+\pi^-\gamma$ final state.

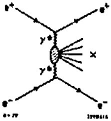

Fig. 1. Diagram for the two-photon production of the state x.

The production cross section of a resonance R by the two-photon interaction is directly proportional to its radiative width $\Gamma_{\gamma\gamma}(R)$ as has been pointed out by Low.[6] Measurements of $\Gamma_{\gamma\gamma}(R)$ allow an interesting direct confrontation of experiments with quark model calculations,[7] especially in the case of the η' meson.[8]

After a short description of the Mark II detector we will present here preliminary results on reaction (1) including all the data accumulated at SPEAR for beam energies E_b above 1.95 GeV. This represents an increase in the integrated luminosity of about a factor 3 over the previously published data sample.[5] We have searched for the following final states from two-photon resonance production: $f(1270) \rightarrow \rho^0\gamma$, $A_2(1310) \rightarrow \rho^{\pm}\pi^{\mp}$ and $f(1270)$, $A_2(1310)$ or $f'(1515)$ decaying into K^+K^-. No signal has been found. Upper limits on the radiative width of these resonances have been obtained from these measurements which will be described in the last chapter.

II. The Mark II Detector

A schematic view of the SLAC-LBL Mark II magnetic detector is shown in Fig. 2. Its configuration and performance have been described elsewhere.[5,9] The detector consists essentially of a large cylindrical drift chamber with 16 layers followed by time-of-flight (TOF) scintillation counters, both embedded in a solenoidal magnet, which in turn is surrounded by a liquid argon electromagnetic shower calorimeter (LA) and a muon detection system. Additional shower counters cover both ends of the cylindrical detector.

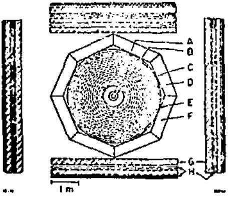

Fig. 2. Schematic view of the Mark II detector. (A) vacuum chamber, (B) pipe counter, (C) drift chamber, (D) time-of-flight counters, (E) solenoid coil, (F) liquid argon shower counters, (G) iron absorber, and (H) muon proportional tubes.

The performance features may be summarized as follows. The azimuthal coordinates for charged tracks are measured in the drift chamber to a rms accuracy of about 210 μm per layer. The magnetic field is 4.1 kG, and when tracks are constrained to pass through the known beam position the momenta of charged particles are determined with a resolution $\delta p/p = \pm[(0.005p)^2 + (0.0145)^2]^{1/2}$ where p is the momentum in GeV/c. The rms time-of-flight resolution for hadrons is 300 ps which provides a π vs. K separation at the one standard deviation level at momenta of 1.35 GeV/c and K vs. p at 2.0 GeV/c. The rms energy resolution for photons and electrons in the liquid argon calorimeter has been measured to be $\delta E/E = 0.11/\sqrt{E}$ (E in GeV) at high energies ($E \gtrsim 0.5$ GeV) and slightly worse ($0.13/\sqrt{E}$) at lower energies because of the increasing importance of the energy loss in the 1.36 radiation lengths of material (coil and supports) in front of the calorimeter. The rms angular resolution is about 8 mrad both in azimuth and dip angle for low energy photons. The measured photon detection efficiencies are

15% at 100 MeV, 50% at 200 MeV and ≥90% above 400 MeV, exclusive of geometry. The LA detector is also used for electron-pion separation. Pion misidentification probabilities of less than 4% and electron efficiencies above 77% are achieved for particle momenta greater than 500 MeV/c. These improve at higher momenta. Finally, muons are detected above $p \sim 700$ MeV/c with a segmented steel hadron absorber. The fraction of the full solid angle covered by the drift chamber and the TOF counters is 75%, by the LA detector is 65%, and by the muon detection system is 55%.

A two stage hardware trigger[10] has been used to select, with efficiency ≥99%, all interactions that have at least one charged particle with transverse momentum $p_\perp > 100$ MeV/c, such that it traverses the entire drift chamber, and another particle which passes through at least the first five layers.

III. Measurement of the Two-Photon Production of the η'

First results on reaction (1) have been reported recently from the Mark II experiment.[5] In the following analysis we have used the same method with similar event selection criteria. All data accumulated at beam energies E_b above 1.95 GeV have been used; the results presented here include the previously published data sample.

The events searched for were $\eta' \to \pi^+\pi^-\gamma$ decays with no additional final state particles detected. The outgoing e^+ and e^- in reaction (1) were not detected. Therefore, events were selected which have only two oppositely charged tracks coming from the interaction region and one photon measured in the LA detector.

The charged particles were identified as pions if their TOF was within 3 standard deviations of the expected time, they deposited less energy in the LA than that expected for electrons, and there were no track-associated hits in the muon chambers behind the hadron absorber. Only those events with an invariant $\pi^+\pi^-$ pair mass of less than 1 GeV/c^2, with each pion momentum less than 1 GeV/c, and with a photon energy E_γ within $0.180 < E_\gamma < 1.0$ GeV have been considered further. With the lower photon energy cut we have removed background that is generated by electronic noise fluctuations (spurious photons).

Kinematical cuts have then been applied to reduce the contributions from the following two main background sources. Possible background from one photon e^+e^- annihilation events with some of the final state particles not detected has been decreased by requiring that the transverse momentum $p_\perp$ of the $\pi^+\pi^-\gamma$ state be less than 250 MeV/c and that the acoplanarity angle $\Delta\phi$ between the $\pi^+\pi^-$ and the γ momentum vectors projected into a plane perpendicular to the beam axis be less than 20^0 ($\Delta\phi = 0^0$ for back-to-back decays). The background from lepton or pion pairs produced in two-photon interactions combined with noise-generated spurious photons was suppressed by requiring that the transverse momentum of the $\pi^+\pi^-$ state be larger than 50 MeV/c and that the acoplanarity angle between the two pions be larger than 3^0.

The $\pi^+\pi^-\gamma$ invariant mass distribution $m_{\pi^+\pi^-\gamma}$ for the events which satisfy all the selection criteria is shown in Fig. 3(a). There is a clear signal of events with an $\eta' \to \pi^+\pi^-\gamma$ decay detected. The observed width of about 40 MeV/c (rms) for the η' mass signal is mostly due to the photon energy resolution and agrees well with a Monte Carlo calculation. The shift of the η' signal by ~25 MeV/c^2 towards higher masses is caused by the steep rise of the photon detection efficiency as a function of the deposited energy in the LA for energies below 400 MeV. This mass shift can be investigated experimentally in the following way. Resonances produced in two-photon interactions at SPEAR energies occur mainly at very low transverse momenta $p_\perp$ with respect to the axis of the colliding electron beams. This fact can be exploited by constraining the events to zero net $p_\perp$ and using a calculated photon energy instead of the measured one. This procedure reduces the expected mass resolution for the η' signal to about 15 MeV/c^2 (rms) and removes the mass shift. However, for events with an η' produced with non-zero $p_\perp$ it gives a wrong mass value. The mass distribution with the constraint $p_\perp = 0$ is shown in Fig. 3(b) for the η' region and displays the expected features.

The only explicit cut applied on the dipion mass has been $m_{\pi\pi} < 1$ GeV/c^2. We find that the dipion mass distribution for the events in the η' mass region, defined as $900 < m_{\pi\pi\gamma} < 1050$ MeV/c^2, is compatible with the hypothesis that all pairs in the $\eta' \to \pi^+\pi^-\gamma$ signal come from ρ^0 decays.

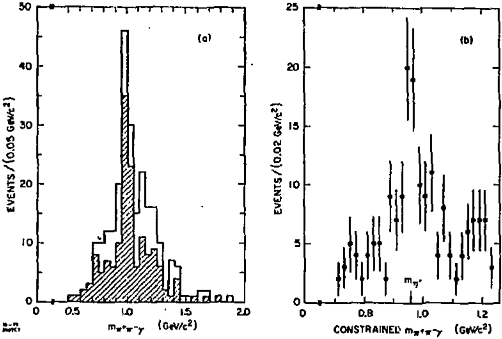

Fig. 3. (a) $\pi^+\pi^-\gamma$ invariant mass distribution. Events from beam energies equal or above 2.6 GeV are shown shaded. (b) $\pi^+\pi^-\gamma$ invariant mass distribution with $p_\perp = 0$ constraint.

The kinematics of two-photon reactions are very characteristic and different from other processes. For the η' produced by reaction (1) the kinematics are distinct, for example, from those of mesons in multi-hadron events from one photon e^+e^- annihilation reactions. The transverse momentum $p_\perp$ distribution is shown in Fig. 4 for all the data (full histogram) and for the subsample of events lying in the η' mass region (shaded). The η' mesons have lower $p_\perp$ than the background events. The distribution of the total energy E is shown in Fig. 5. The energy of η' appears to be confined to low values, excluding the possibility that the η' is produced in a two-body annihilation reaction like $\eta'\gamma$ with the γ not detected. The angular distribution of the η' mesons is strongly peaked along the beams. Their rapidity (y) distribution, given in Fig. 6, is flat over the whole detector acceptance of about $-0.5 < y < 0.5$, whereas the background events tend to peak around $y = 0$.

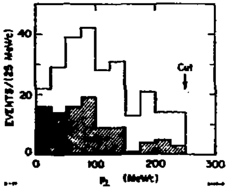

Fig. 4. Transverse momentum distribution. Events in the η' peak $0.90 < m_{\pi^+\pi^-\gamma} < 1.05$ GeV/c^2 are shaded.

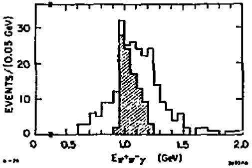

Fig. 5. Total energy distribution. Events in the η' peak $0.90 < m_{\pi^+\pi^-\gamma} < 1.05$ GeV/c^2 are shaded.

The background has been studied with two different methods. In the first method we have analyzed multihadron e^+e^- annihilation events. The same analysis cuts as for reaction (1) except for the topology selection have been applied to events with three or more charged prongs and at least one photon. The resulting mass distribution is smooth and reaches a broad maximum over the range from 0.8 to 1.3 GeV/c^2. The transverse momentum distribution rises below about 125 MeV/c and stays approximately constant above. In the second method we have used all the original selection criteria including the exclusive two-charged prongs and only one photon topology but have then

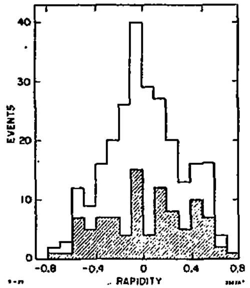

Fig. 6. Rapidity distribution for the $\pi^+\pi^-\gamma$ states, with the events in the η' peak shaded.

combined the dipion state from one event with the photon from the next event. This analysis reproduces the shape and the normalization of the observed background in the mass and transverse momentum distributions. Both these studies suggest a smooth background shape under the η' signal, and we have therefore made a direct subtraction using the adjacent mass regions (see Table I). This subtraction makes no specific assumptions on the origin of the background. We notice that the background contribution is lower for the data taken at the higher beam energies than for the low energy part of the data (see Fig. 3(a)).

TABLE I

Summary of the Cross Section Calculation

E_b (GeV)	$\int \mathcal{L} dt$ (nb^{-1})	ε	$n_{\eta'}$	$\sigma(\eta')$ (nb)
1.95–2.21	4199	0.0231	7.7 ± 5.1	0.27 ± 0.18
2.25–2.50	2131	0.0224	4.3 ± 2.6	0.30 ± 0.18
2.50–3.00	6655	0.0211	25.9 ± 7.1	0.62 ± 0.17
3.00–3.35	4009	0.0177	20.0 ± 5.9	0.94 ± 0.28
3.70	984	0.0125	3.1 ± 2.2	0.84 ± 0.60

E_b is the beam energy, $\int \mathcal{L} dt$ is the integrated luminosity, ε is the detection efficiency not including $B(\eta' \to \pi\pi\gamma)$, $n_{\eta'}$ is the background subtracted number of η' events and $\sigma(\eta')$ is the observed cross section. Only statistical errors are shown.

The cross section has been calculated using the detection efficiency ε for reaction (1) and the branching ratio $B(\eta' \to \pi^+\pi^-\gamma) = 0.298 \pm 0.017$.[11] The detection probability has been determined by a Monte Carlo simulation. Events have been generated according to the cross section calculation and angular distribution of Ref. 12. These events have then been subject to the same detector geometry and selection criteria as the real data except for the LA shower cuts on the charged tracks. Because of the difficulties of describing in detail the interaction of pions in the shower counter material, the efficiencies of the latter cuts (typically 85%) have been determined experimentally with unambigously identified pions from ϕ decays. Furthermore, there is a small (5%) loss of events due to additional spurious photons which has also been determined experimentally. The observed cross section $\sigma(\eta')$, and ε, are given in Table I. The cross section $\sigma(\eta')$ is also displayed in Fig. 7 as a function of the beam energy and is found to be compatible with the expected slow rise with increasing energy. The errors shown for $\sigma(\eta')$ are statistical only and do not include an estimated overall systematic uncertainty of ±20%. We have not corrected the displayed cross sections for initial state radiation in reaction (1).

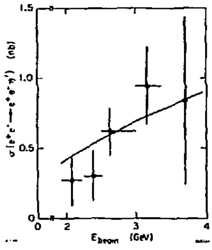

Fig. 7. Cross section for $e^+e^- \to e^+e^-\eta'$ as a function of the beam energy. The curve is the result of Eq. (2) with $\Gamma_{\gamma\gamma}(\eta') = 6$ keV.

The two-photon production cross section for a resonance R is directly proportional to the radiative width $\Gamma_{\gamma\gamma}(R)$ of the resonance.[6] This can be seen for example in the equivalent photon approximation calculation of Ref. 13

$$\sigma_{ee\to eeR} = 16\alpha^2(2J+1)\, m_R^{-3}\, \Gamma_{\gamma\gamma}(R) \times \left(\ln\frac{E_b}{m_e} - \frac{1}{2}\right)^2 f\left(\frac{m_R}{2E_b}\right) \qquad (2)$$

with

$$f(x) = (2+x^2)^2 \ln\frac{1}{x} - (1-x^2)(3+x^2) \quad .$$

J denotes the spin and m_R the mass of the resonance. E_b is the beam energy and m_e the electron mass. From the measured cross section for reaction (1) we have determined $\Gamma_{\gamma\gamma}(\eta') = 5.8 \pm 1.1$ keV using the two-photon calculation of Ref. 12. In this calculation we have included the correction for initial state radiation effects. The error reflects the statistical accuracy of the measurement but does not include an estimated overall systematic uncertainty of ±20%. Upper limits on $\Gamma_{\gamma\gamma}(\eta')$ in the range 11 to 35 keV had been obtained in other searches[2-4] for reaction (1). From the radiative width we have deduced the total width $\Gamma_{tot}(\eta') = 293 \pm 67$ keV (±20% systematic uncertainty) using the $B(\eta' \to \gamma\gamma) = 0.0197 \pm 0.0026$.[11] This measurement of $\Gamma_{tot}(\eta')$ is in good agreement with the value 280 ± 100 keV reported in Ref. 14.

The radiative width for the η' has been calculated by several authors[8,15,16] as will be discussed by F. J. Gilman in the following talk.[7] In short, quark models with fractionally charged quarks lead, under the assumptions of a small pseudoscalar octet-singlet mixing angle and of equal singlet and octet decay constants, to the prediction of $\Gamma_{\gamma\gamma}(\eta') \sim 6$ keV in very good agreement with our measurement. Applying the same assumptions, the data is not compatible with integral charge quark models, for which a radiative decay width of about 26 keV is predicted. However, the validity of these assumptions has been questioned in Ref. 15 where alternative analyses are proposed.

IV. Upper Limits on the Radiative Widths of the Tensor Mesons f, A_2 and f'

The radiative widths of the tensor mesons f(1270), A_2(1310) and f'(1515) are experimentally not known. From SU(3) symmetry they are expected to have values in the ratio 25:9:2 for the case of ideal mixing and with phase space corrections neglected.[7] The $\Gamma_{\gamma\gamma}$ for the f(1270) meson has been calculated by several authors, see for example Refs. 17 and 18, which predict $\Gamma_{\gamma\gamma}(f)$ to be in the range of about 5 to 20 keV.

We have investigated exclusive final states for the following reactions

$$e^-e^- \to e^+e^- \, f(1270) \hookrightarrow \rho^0\gamma \tag{3}$$

$$e^+e^- \to e^+e^- \, A_2(1310) \hookrightarrow \rho^\pm\pi^\mp \tag{4}$$

$$e^+e^- \to e^+e^- \, f(1270) \hookrightarrow K^+K^- \tag{5}$$

$$e^+e^- \rightarrow e^+e^- A_2(1310) \quad (6)$$
$$\qquad \qquad \llcorner\!\!\rightarrow K^+K^-$$

$$e^+e^- \rightarrow e^+e^- f'(1515) \quad (7)$$
$$\qquad \qquad \llcorner\!\!\rightarrow K^+K^-$$

$$e^+e^- \rightarrow e^+e^- f(1270) \quad (8)$$
$$\qquad \qquad \llcorner\!\!\rightarrow \pi^+\pi^-$$

by searching for signals in the invariant mass distributions of the respective final states which would occur at low transverse momenta. As in the measurement of reaction (1), the final state $e^+$and e^- remained undetected. No signal above background has been detected for reactions (3) to (7). We have used the data taken at beam energies above 2.25 GeV (14 pb^{-1} integrated luminosity) to determine upper limits on the radiative widths of these tensor mesons as described below. The study of final state pion pairs from two-photon interactions, including reaction (8) and the direct process $e^+e^- \rightarrow e^+e^-\pi^+\pi^-$, is not yet completed.

A. $\rho^0\gamma$ Final State

It has been recently proposed[10] that the f(1270) meson could have a relatively large branching fraction into $\rho^0\gamma$, namely 3 to 5%. We have searched for reaction (3) using the same method as described in the preceding chapter for the measurement of reaction (1). The same cuts have been applied except that the lower photon energy cut has been increased to 250 MeV in order to further suppress backgrounds. The resulting $\pi^+\pi^-\gamma$ mass distribution is shown in Fig. 8(a) and the $p_\perp$ distribution in Fig. 8(b) with the events from the mass interval $1.15 < m_{\pi\pi\gamma} < 1.40$ GeV/c^2 shaded. No signal at the f(1270) mass is present. The η' signal appears reduced due to the more stringent photon energy cut. The background mass distribution can be well described with artifically generated events in which the dipion state has been combined with the photon from the next event of the same two charged prongs and only one photon topology. The overall detection efficiency for reaction (3) has been determined in the same way as for reaction (1) and found to be 0.020. The data therefore allow us to set a 95% C.L. upper limit on the product $\sigma(f) \times B(f \rightarrow \rho\gamma) < 0.14$ nb at the luminosity-weighted average beam energy of 2.85 GeV. With Eq. (2) this equates to $\Gamma_{\gamma\gamma}(f) \times B(f \to \rho\gamma) < 0.8$ keV. Both limits include an estimated 20% systematic uncertainty.

B. $\rho^{\pm}\pi^{\mp}$ Final State

To search for reaction (4), we have selected the event topology which contains two oppositely charged pions and two photons. All events with two photons in the energy range $0.1 < E_{\gamma} < 1.0$ GeV and with a two-photon invariant mass $m_{\gamma\gamma}$ within $0.075 < m_{\gamma\gamma} < 0.200$ GeV/c^2 have been selected. For these events the photon energies were adjusted to constrain $m_{\gamma\gamma}$ to m_{π^0}. These π^0 have been combined with either one of the charged pions to form the invariant mass $m_{\pi^{\pm}\pi^0}$. Only those events with a $\rho^{\pm}$ candidate, defined as $0.5 < m_{\pi^{\pm}\pi^0} < 1.0$ GeV/c^2, have been retained any further. Special cuts have been necessary to suppress the background coming from τ lepton pair production with their subsequent decays into $\rho^{\pm}\nu_{\tau}$ and final states containing single or multipions which have been measured in the same experiment.[19] Both the $\rho^{\pm}$ and the $\pi^{\mp}$ momenta have been required to be less than 800 MeV/c. Finally, the invariant $\rho^{\pm}\pi^{\mp}$ mass has been formed, and a transverse momentum cut of $p_{\perp} < 250$ MeV/c on it has been applied to reduce the background from one photon e^+e^- annihilation events. The $m_{\rho^{\pm}\pi^{\mp}}$ and $p_{\perp}$ distributions are shown in Figs. 9(a) and 9(b), with the events lying in the A_2 mass region $1.20 < m_{\rho^{\pm}\pi^{\mp}} < 1.45$ GeV/c^2 shaded in

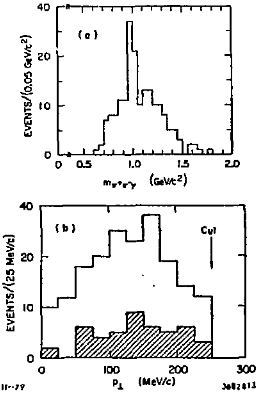

Fig. 8. (a) $\pi^+\pi^-\gamma$ invariant mass distribution for the $f(1270) \to \rho^0\gamma$ search. (b) Transverse momentum distribution; events from the f(1270) mass region $1.15 < m_{\pi^+\pi^-\gamma} < 1.40$ GeV/c^2 are shaded.

Fig. 9(b). From the observed background in the $m_{\rho^\pm\pi^\mp}$ distribution, the known $B(A_2 \to \rho^\pm\pi^\mp) = 0.703 \pm 0.021$ [11] and the overall detection efficiency for reaction (4) $\epsilon = 0.0028$, which is greatly reduced due to the low energy photon efficiency, one deduces a 95% C.L. upper limit for $\sigma(A_2) < 0.36$ nb at $E_b = 2.85$ GeV for reaction (4). From Eq. (2) it follows that $\Gamma_{\gamma\gamma}(A_2) < 2.5$ keV. A possible systematic error of 25% has been included in these limits.

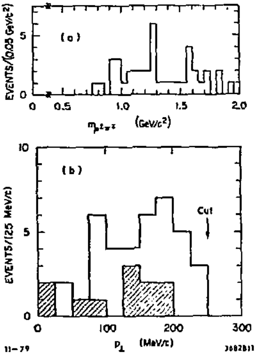

Fig. 9. (a) $\rho^\pm\pi^\mp$ invariant mass distribution. (b) Transverse momentum distribution; events from the $A_2(1310)$ mass region $1.20 < m_{\rho^\pm\pi^\mp} < 1.45$ GeV/c^2 are shaded.

C. K^+K^- Final State

The K^+K^- decay modes of the f(1270), A_2(1310) and f'(1515) mesons can be used to study their two-photon production with little background from one photon e^+e^- annihilation processes. For this purpose we have selected events with only two oppositely charged prongs and no detected photons. Both tracks have been required to be unambigously identified as kaons by the TOF measurement. This has been achieved by a cut on the probability level[20] which has been required to be larger than 0.65 for both tracks to be a kaon. In order to reduce sources other than two-photon production we have applied two loose kinematical cuts: the acoplanarity angle $\Delta\phi$ between the two kaons had to be $<20^\circ$ and the $p_\perp$ of the K^+K^- state had to be <250 MeV/c. The invariant mass $m_{K^+K^-}$ and the $p_\perp$ distributions are given in Figs. 10(a) and 10(b). The $p_\perp$ of most of the events is seen to be very small as expected for reactions (5) to (7).

Non-resonant production can also contribute to K^+K^- final states from two-photon interactions. We have estimated the expected background in the $m_{K^+K^-}$ distribution from the nonresonant process

$$e^+e^- \rightarrow e^+e^-K^+K^- \qquad (9)$$

with the equivalent photon approximation of Ref. 21. The curve in Fig. 10(c) shows the result of using a simple kaon form factor with a Φ pole of the form $|F_K(s)| = (1 - s/m_\phi^2)^{-1}$. With this assumption for the form factor the contribution of reaction (9) appears to be small (10% over the range of observed K^+K^- masses). The low statistics of the data in Fig. 10(a) only allows us to extract upper limits on the production cross sections for the f(1270) and A_2(1310) mesons in reactions (5) and (6), where we have used the branching ratios[11] into K^+K^- of 0.0165 ± 0.002 and 0.0235 ± 0.0025 and overall detection efficiencies of 0.0167 and 0.0172, respectively, at the average beam energy of 2.85 GeV. The results as well as the upper limits on $\Gamma_{\gamma\gamma}$ from Eq. (2) are given in Table II. The branching ratio of the f'(1515) meson into $K\bar{K}$ is not known, but expected to be dominant[11] (i.e., $B(f' \rightarrow K^+K^-)$ near 0.5). The data together with

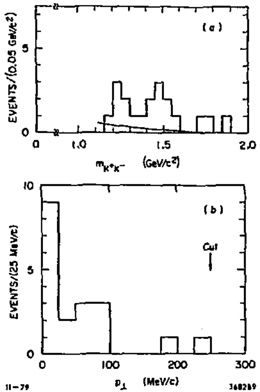

Fig. 10. (a) Invariant K^+K^- mass distribution. The curve shows the expected contribution from nonresonant two-photon interactions (see text). (b) Transverse momentum distribution of the K^+K^- system.

TABLE II

Final State	Meson	ϵ	σ (nb)	$\Gamma_{\gamma\gamma}$ (keV)
$\rho^o\gamma$	f(1270)	0.0200	$\sigma \times B(f \to \rho\gamma)$ < 0.14	$\Gamma_{\gamma\gamma} \times B(f \to \rho\gamma)$ < 0.8
$\rho^{\pm}\pi$	$A_2(1310)$	0.0028	< 0.36	< 2.5
K^+K^-	f(1270)	0.0167	< 4.2	< 24.0
K^+K^-	$A_2(1310)$	0.0172	< 2.6	< 17.0
K^+K^-	f'(1515)	0.0195	$\sigma \times B(f' \to K^+K^-)$ < 0.052	$\Gamma_{\gamma\gamma} \times B(f' \to K^+K^-)$ < 0.6

Upper limits (95% C.L.) on the two-photon production cross section σ and the radiative width $\Gamma_{\gamma\gamma}$ of the tensor mesons at the luminosity weighted average beam energy 2.85 GeV. The overall detection efficiency is listed under ϵ and B stands for branching ratio.

the calculated detection efficiency of 0.0195 provides therefore only upper limits on $B(f' \to K^+K^-) \times \sigma(f')$ and $B(f' \to K^+K^-) \times \Gamma_{\gamma\gamma}(f')$ for reaction (7). These upper limits are also listed in Table II. A systematic uncertainty for the K^+K^- final states of 15% has been included in the listed 95% C.L. upper limits.

We have summarized in Table II the upper limits on the radiative widths of the f(1270), $A_2(1310)$ and f'(1515) mesons obtained from the final states studied so far. All of these limits are consistant with the expected values mentioned at the beginning of this chapter.

We wish to thank Drs. S. J. Brodsky and F. J. Gilman for stimulating discussions.

V. References and Footnotes

1. V. E. Balakin et al., Phys. Lett. 34B, 663 (1971); C. Bacci et al., Nuovo Cimento Lett. 3, 709 (1972); G. Barbiellini et al., Phys. Rev. Lett. 32, 385 (1974).

2. H. J. Besch et al., Phys. Lett. 81B, 79 (1979); A. Courau et al., Phys. Lett. 84B, 145 (1979).

3. Ch. Berger et al., Phys. Lett. 81B, 410 (1979); R. Baldini Celio et al., Phys. Lett. 86B, 239 (1979).

4. S. Orito et al., Phys. Lett. 48B, 380 (1974); L. Paoluzi et al., Nuovo Cimento Lett. 10, 435 (1974).

5. G. S. Abrams et al., Phys. Rev. Lett. 43, 477 (1979).

6. F. E. Low, Phys. Rev. 120, 582 (1960).

7. See for example, F. J. Gilman, Proc. of Internat. Conf. on Two-Photon Interactions, Lake Tahoe, California 1979.

8. S. Matsuda and S. Oneda, Phys. Rev. 187, 2107 (1969); S. Okubo, in "Symmetries and Quark Models," R. Chand, ed., Gordon and Breach, New York (1970); H. Suura, T. F. Walsh and B-L. Young, Nuovo Cimento Lett. 4, 505 (1972).

9. W. Davies-White et al., Nucl. Instrum. Methods 160, 227 (1979); G. S. Abrams et al., IEEE Trans. on Nucl. Sci., NS-25, 309 (1978).

10. H. Brafman et al., IEEE Trans. on Nucl. Sci. NS-25, 692 (1978).

11. Compiled by Particle Data Group, Phys. Lett. 75B, 1 (1978).

12. V. M. Budnev and I. F. Ginzburg, Phys. Lett. 37B, 320 (1971); V. N. Baier and V. S. Fadin, Nuovo Cimento Lett. 1, 481 (1971), and private communication.

13. S. J. Brodsky, T. Kinoshita and H. Terazawa, Phys. Rev. Lett. 25, 972 (1970) and Phys. Rev. D4, 1532 (1971).

14. D. M. Binnie et al., Phys. Lett. 83B, 141 (1979).

15. M. S. Chanowitz, Phys. Rev. Lett. 35, 977 (1975) and Lawrence Berkeley Laboratory preprint LBL-9639 (1979).

16. E. Etim and M. Greco, Nuovo Cimento 42, 124 (1977); N. M. Chase and M. T. Vaughn, Z. Physik C 2, 23 (1979).

17. B. Renner, Nucl. Phys. B30, 634 (1971); B. Schrempp-Otto, F. Schrempp and T. F. Walsh, Phys. Lett. 36B, 463 (1971).

18. W. N. Cottingham and I. H. Dunbar, H. H. Wills Physics Laboratory, University of Bristol, Bristol, U.K. (1979), preprint.

19. G. S. Abrams et al., SLAC-PUB-2365 (1979), submitted to Phys. Rev. Lett.

20. Each track is assigned weights for being a pion, kaon or proton. Each weight is proportional to the probability that if the particle has the assumed identity, its flight time would have the measured value. The normalization is such that the sum of all weights for a given track is unity.

21. S. J. Brodsky, Suppl. J. Phys., tome 35, page C2-69 (1974) and Ref. 12.